

Dynamic Modeling and Computer Simulation for Autonomous Underwater Vehicles with Fins

Xiao Liang¹

College of Traffic Equipment and Ocean Engineering, Dalian Maritime University, Dalian, China

Email: liangxiao19801012@126.com

Jundong Zhang², Yu Qin¹ and Hongrui Yang³

College of Traffic Equipment and Ocean Engineering, Dalian Maritime University, Dalian, China

College of Marine Engineering, Dalian Maritime University, Dalian, China

College of Information Science and Engineering, Northeastern University, Shenyang, China

Email: zhjundong@126.com, qinyu.favor@hotmail.com, hr1992@21cn.com

Abstract—The application of autonomous underwater vehicles (AUV) is widespread with the development of the activities in deep sea. For low energy consumption, low resistance and excellent maneuverability, fins are usually used to modify AUV hydrodynamic forces. The AUV with fins can do gyratory motion by vertical fins and do diving and rising motion by horizontal fins. However, the modeling and motion control of the AUV with fins have not been solved well, which this paper concentrates on. Firstly, we build the motion equation in six degree of freedom and analyze the forces and hydrodynamic coefficients in detail, especially the fin effect. The feasibility and accuracy are verified by comparing the results between ocean experiments and simulation on WL-II mini-AUV.

Index Terms—autonomous underwater vehicle, dynamic modeling, fins, simulation

I. INTRODUCTION

With the development of the activities in deep sea, application of the AUV is widespread, and there is a very prominent prospect. The research on the AUV includes many areas, such as vehicle (carrier/platform) design, architecture, motion control, intelligent planning and decision making, etc [1-3]. Researchers dedicate themselves to improving the performance on modularization, low-cost AUV in such applications as long-range oceanographic survey, autonomous docking, and shallow-water mine countermeasures. These goals can be achieved through the improvement of maneuvering precision and motion control capability with energy constraints. For low energy consumption, low resistance, and excellent maneuverability, fins are usually used to modify AUV hydrodynamic force. The AUV with fins can do gyratory motion by vertical fins and do diving and rising motion by horizontal fins. Therefore, the control system of the propeller-fin-driven AUV is very different to the conventional only-propeller-driven AUV.

A dynamic mathematic model for the AUV with fins based on a combination of theory and empirical data

would provide an efficient platform for control system development, and an alternative to the typical trial-and-error method of control system tuning. Although some modeling and simulation methods have been proposed and applied [4, 5, 8-11], there is no standard procedure for modeling the AUV with fins in industry. Therefore, the modeling and simulation of the AUV with fins is a challenge.

This paper describes the development and verification of a six degree of freedom (DOF), non-linear model for the AUV with fins. In the model, the external force and moment resulting from hydrostatics, hydrodynamic lift and drag, added mass, and the thrusters and fins are all analyzed and expressed in matrix form. The equations describing the rigid-body dynamics are left in non-linear form to better simulate the AUV inherently non-linear behavior. Motion simulation is achieved through numeric integration of the motion equations. The simulation output is then checked with the AUV dynamics data collected in experiments at sea. The comparison results show that the non-linear model gives an accurate estimation to the actual motion of the AUV. The research object is WL-II mini-AUV, which is a small, low-cost platform serving in a range of oceanographic applications [12].

II. MATHEMATIC MODELLING OF AUV MOTION

A. Coordinate System and Motion Parameters Definition

It is convenient to analyze the equations of the rigid-body motion respecting to a body-fixed reference frame which keep the body geometry invariant all the time. Basing on the recommendation of International Towing Tank Conference (ITTC) and the Society of Naval Architects and Marine Engineers (SNAME), we build two reference coordinates. Start with the application of Newton II law to the AUV motion by a fixed inertial frame of reference $E - \zeta\eta\varsigma$ (global coordinates), and then transfer the equations to the body-fixed coordinates (local

coordinates) $o-xyz$ through coordinate transformation relation. We can obtain 6-DOF equations of the rigid-body motion referred to as surge, sway, heave, roll, pitch and yaw. The global coordinates and local coordinates are illustrated in figure 1.

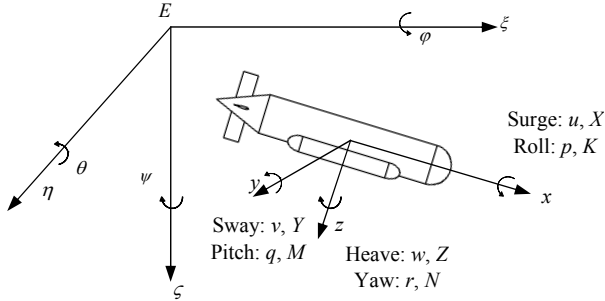


Figure 1. Body-fixed and inertial coordinate system.

Considering shape characteristics for most AUVs, the mathematic model is basing on the hypothesis that the AUV is symmetric on the xoz plane.

Defining generalized position vector \mathbf{R} , generalized velocity vector \mathbf{V} and generalized force vector $\boldsymbol{\tau}$, the motion vector include

(1) Position and attitude (in $E-\zeta\eta\zeta$)

$$\mathbf{R} = [\mathbf{r}^T, \boldsymbol{\Lambda}^T]^T, \mathbf{r} = [\zeta, \eta, \zeta]^T, \boldsymbol{\Lambda} = [\varphi, \theta, \psi]^T$$

(2) Linear and angular velocities (in $o-xyz$)

$$\mathbf{C}_{RB}(\mathbf{V}) = \begin{bmatrix} 0 & -mr & mq & m(y_G q + z_G r) & -mx_G q & -mx_G r \\ mr & 0 & -mp & -my_G p & m(z_G r + x_G p) & -my_G r \\ -mq & mp & 0 & -mz_G p & -mz_G q & m(x_G p + y_G q) \\ -m(y_G q + z_G r) & my_G p & mz_G p & 0 & J_{zx} p + J_{zy} q + J_z r & -J_{yx} p - J_y q - J_{yz} r \\ mx_G u & -m(z_G r + x_G p) & mz_G q & -J_{zx} p - J_{zy} q - J_z r & 0 & J_x p + J_{xy} q + J_{xz} r \\ mx_G r & my_G r & -m(x_G p + y_G q) & J_{yx} p + J_y q + J_{yz} r & -J_x p - J_{xy} q - J_{xz} r & 0 \end{bmatrix} \quad (3)$$

Generalized force vector $\boldsymbol{\tau}$ at the right of (1) is outside force (or moment) acting on the AUV, including static force vector $\boldsymbol{\tau}_G$ (gravity and buoyancy), hydrodynamics force vector of the vehicle body (include $\boldsymbol{\tau}_A$ which is caused by added mass and viscous damping force $\boldsymbol{\tau}_V$), and the controlled force vector

$$\boldsymbol{\tau}_G = \begin{bmatrix} X_G \\ Y_G \\ Z_G \\ K_G \\ M_G \\ N_G \end{bmatrix} = \begin{bmatrix} -(W - B) \cdot \sin \theta \\ (W - B) \cdot \sin j \cos \theta \\ (W - B) \cdot \cos j \cos \theta \\ (y_G W - y_B B) \cdot \cos j \cos \theta - (z_G W - z_B B) \cdot \sin j \cos \theta \\ -(x_G W - x_B B) \cdot \cos j \cos \theta - (z_G W - z_B B) \cdot \sin \theta \\ (x_G W - x_B B) \cdot \sin j \cos \theta - (y_G W - y_B B) \cdot \sin \theta \end{bmatrix} \quad (4)$$

Where x_B, y_B, z_B are the vehicle coordinates in body-fixed coordinate system.

$\boldsymbol{\tau}_A$ which is related with added mass is given by

$$\boldsymbol{\tau}_A = -(\mathbf{M}_A \dot{\mathbf{V}} + \mathbf{C}_A(\mathbf{V})\mathbf{V}) \quad (5)$$

Where \mathbf{M}_A is the added mass matrix, which is given by

$$\mathbf{V} = [\mathbf{U}^T, \boldsymbol{\Omega}^T]^T, \mathbf{U} = [u, v, w]^T, \boldsymbol{\Omega} = [p, q, r]^T$$

(3) Force and moment parameters (in $o-xyz$)

$$\boldsymbol{\tau} = [\mathbf{F}^T, \mathbf{M}^T]^T, \mathbf{F} = [X, Y, Z]^T, \mathbf{M} = [K, M, N]^T$$

B. Dynamics Model

Basing on momentum theorem, the AUV dynamic equation is

$$\mathbf{M}_{RB} \dot{\mathbf{V}} + \mathbf{C}_{RB}(\mathbf{V})\mathbf{V} = \boldsymbol{\tau} \quad (1)$$

Where \mathbf{M}_{RB} is the generalized mass matrix of the vehicle body, and $\mathbf{C}_{RB}(\mathbf{V})$ is the Coriolis and centripetal force matrix. \mathbf{M}_{RB} is given by

$$\mathbf{M}_{RB} = \begin{bmatrix} m & 0 & 0 & 0 & mz_G & -my_G \\ 0 & m & 0 & -mz_G & 0 & mx_G \\ 0 & 0 & m & my_G & -mx_G & 0 \\ 0 & -mz_G & my_G & J_x & J_{xy} & J_{xz} \\ mz_G & 0 & -mx_G & J_{yx} & J_y & J_{yz} \\ -my_G & mx_G & 0 & J_{zx} & J_{zy} & J_z \end{bmatrix} \quad (2)$$

Where m is the AUV mass, J terms represent the inertial tensors, and x_G, y_G, z_G represent the AUV position barycenter in local coordinates. $\mathbf{C}_{RB}(\mathbf{V})$ is given by

(include the thruster force $\boldsymbol{\tau}_{prop}$ and the fin force $\boldsymbol{\tau}_R$).

The static force vector $\boldsymbol{\tau}_G$ reflects the effect of the vehicle weight and buoyancy. The vehicle weight is $W = mg$ and the buoyancy is $B = \rho \nabla g$, where ρ is the density of the surrounding fluid, and ∇ is the total volume displaced by the AUV. Therefore, $\boldsymbol{\tau}_G$ is given by

$$\mathbf{M}_A = \begin{bmatrix} \lambda_{11} & 0 & \lambda_{13} & 0 & \lambda_{15} & 0 \\ 0 & \lambda_{22} & 0 & \lambda_{24} & 0 & \lambda_{26} \\ \lambda_{31} & 0 & \lambda_{33} & 0 & \lambda_{35} & 0 \\ 0 & \lambda_{42} & 0 & \lambda_{44} & 0 & \lambda_{46} \\ \lambda_{51} & 0 & \lambda_{53} & 0 & \lambda_{55} & 0 \\ 0 & \lambda_{62} & 0 & \lambda_{64} & 0 & \lambda_{66} \end{bmatrix} \quad (6)$$

Where λ terms represent the vehicle added mass.

\mathbf{M}_A can be also denoted as hydrodynamic coefficients expression:

$$\mathbf{M}_A = \begin{bmatrix} X_{\dot{u}} & 0 & X_{\dot{w}} & 0 & X_{\dot{q}} & 0 \\ 0 & Y_{\dot{v}} & 0 & Y_{\dot{p}} & 0 & Y_{\dot{r}} \\ Z_{\dot{u}} & 0 & Z_{\dot{w}} & 0 & Z_{\dot{q}} & 0 \\ 0 & K_{\dot{v}} & 0 & K_{\dot{p}} & 0 & K_{\dot{r}} \\ M_{\dot{u}} & 0 & M_{\dot{w}} & 0 & M_{\dot{q}} & 0 \\ 0 & N_{\dot{v}} & 0 & N_{\dot{p}} & 0 & N_{\dot{r}} \end{bmatrix} \quad (7)$$

$C_A(\mathbf{V})$ is a Coriolis-like matrix induced by \mathbf{M}_A ,

$$\mathbf{D}(\mathbf{V}) = \begin{bmatrix} X_u + X_{u|u}|u| & 0 & 0 & 0 & 0 & 0 \\ 0 & Y_v + Y_{v|v}|v| & 0 & 0 & 0 & 0 \\ Z_0|u| & 0 & Z_w + Z_{w|w}|w| & 0 & 0 & 0 \\ 0 & 0 & 0 & 0 & 0 & 0 \\ M_0|u| & 0 & 0 & 0 & 0 & 0 \\ 0 & 0 & 0 & 0 & 0 & 0 \end{bmatrix} \quad (10)$$

Where $X_u, Y_v, Z_w, K_p, M_q,$ and N_r are the linear damping coefficients. $Y_{v|v}, Z_{w|w}, K_{p|p}, M_{q|q}, X_{u|u},$ and $N_{r|r}$ are the quadratic damping coefficients. M_0 and Z_0 are the effect caused by the dissymmetry on xoy plane.

The external force and moment vector produced by thrusters τ_{prop} is defined as

$$\tau_{prop} = \mathbf{L}\mathbf{T}_{prop} \quad (11)$$

Where \mathbf{L} is a mapping matrix, and \mathbf{T}_{prop} is the thrust vector produced by thrusters given by

$$\mathbf{T}_{prop} = \begin{bmatrix} T_1 \\ T_2 \\ \vdots \\ T_n \end{bmatrix} \quad (12)$$

The number n in \mathbf{T}_{prop} depends on the number of thrusters. The mapping matrix \mathbf{L} is a $6 \times n$ matrix that uses \mathbf{T}_{prop} to find the overall force and moment acting on the vehicle.

Hydrodynamics of a single thruster is usually obtained through the in water test. A series of advance coefficient J corresponding to the thrust coefficient K_T data can be obtained from the in water test. Data from an in water test are shown in Fig.2. We fit the curve by the method of least squares and then obtain the fitted $J - K_T$ curve. In practical applications, we get advance coefficient J

$$C_A(\mathbf{V}) = \begin{bmatrix} 0 & 0 & 0 & 0 & a_3 & -a_2 \\ 0 & 0 & 0 & -a_3 & 0 & a_1 \\ 0 & 0 & 0 & a_2 & -a_1 & 0 \\ 0 & a_3 & -a_2 & 0 & b_3 & -b_2 \\ -a_3 & 0 & a_1 & -b_3 & 0 & b_1 \\ a_2 & -a_1 & 0 & b_2 & -b_1 & 0 \end{bmatrix} \quad (8)$$

Where

$$\begin{cases} a_1 = \lambda_{11}u + \lambda_{13}w + \lambda_{15}q \\ a_2 = \lambda_{22}v + \lambda_{24}p + \lambda_{26}r \\ a_3 = \lambda_{31}u + \lambda_{33}w + \lambda_{35}q \\ b_1 = \lambda_{42}v + \lambda_{44}p + \lambda_{46}r \\ b_2 = \lambda_{51}u + \lambda_{53}w + \lambda_{55}q \\ b_3 = \lambda_{62}v + \lambda_{64}p + \lambda_{66}r \end{cases}$$

The viscous damping force τ_V is given by

$$\tau_V = \mathbf{D}(\mathbf{V})\mathbf{V} \quad (9)$$

The damping matrix $\mathbf{D}(\mathbf{V})$ is given by

$$\begin{bmatrix} 0 & 0 & 0 & 0 & 0 & 0 \\ 0 & 0 & 0 & 0 & 0 & 0 \\ 0 & 0 & 0 & 0 & 0 & 0 \\ K_p + K_{p|p}|p| & 0 & 0 & 0 & 0 & 0 \\ 0 & M_q + M_{q|q}|q| & 0 & 0 & 0 & 0 \\ 0 & 0 & 0 & 0 & N_r + N_{r|r}|r| & 0 \end{bmatrix}$$

and substitute it into fitted $J - K_T$ curve to get K_T . Finally, the thrust can be obtained. Detailed process is as follows:

(1) We get the advance coefficient J from fluid velocity cross the propeller V_{prop} , the propeller diameter D , and the screw propeller rotate speed n (n is determined by controller): $J = \frac{V_{prop}}{nD}$.

(2) We put J into fitted $J - K_T$ curve to get force coefficient K_T .

(3) We get the thrust forces by $\mathbf{T} = K_T n^2 D^4$.

The overall external force and moment vector produced by fins τ_R is given by

$$\tau_R = \begin{bmatrix} X_R \\ Y_R \\ Z_R \\ K_R \\ M_R \\ N_R \end{bmatrix} \quad (13)$$

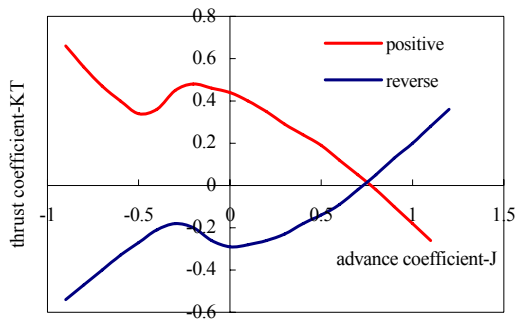


Figure 2. Capability curves of thrusters.

According to every single fin force and the installation position, τ_R can be obtained.

As to a control fin on the vehicle, the hydrodynamic force can be decomposed into two directions: lift force L —vertical to stream current and drag force D —along stream current. Lift force and drag force can be calculated by the following equations:

$$\begin{cases} L = \frac{1}{2} C_L \rho A_R v_e^2 \\ D = \frac{1}{2} C_D \rho A_R v_e^2 \end{cases} \quad (14)$$

Where C_L is the fin lift coefficient, C_D is the fin drag coefficient, A_R is the fin platform area, and v_e is the effective fin velocity. The values of lift coefficient C_L and drag coefficient C_D are related with effective fin angle of attack α .

We can adopt experiment, theory computation, or empirical formula to get C_L and C_D . Experiment and empirical formula method will be introduced below.

(1) Actual measurement from experiment

A series of data of angles of attack α vs. lift coefficient C_L and drag coefficient C_D can be obtained from hydrodynamic experiment, and then fitted curves of C_L and C_D can be generated through least squares fit. For example, the fitted curves of a fin is shown in Fig.3.

When we know the current angle of attack of fin on the AUV, the values of C_L and C_D under this angle can be obtained by curves interpolation.

(2) Method of empirical equation

The empirical equations to calculate C_L and C_D are given by

$$C_L = \frac{\partial C_L}{\partial \alpha} \times \alpha + \frac{C_{DC}}{\lambda} \left(\frac{\alpha}{57.3} \right)^2 \quad (15)$$

$$\frac{\partial C_L}{\partial \alpha} = \frac{0.9(2\pi)\lambda}{57.3[\cos \Lambda \sqrt{\frac{\lambda^2}{\cos^4 \Lambda} + 4 + 1.8}]} \quad (16)$$

$$C_D = C_{d0} + \frac{C_L^2}{\epsilon\pi\lambda} \quad (17)$$

Where $\frac{\partial C_L}{\partial \alpha}$ is the slope at $\alpha=0$ in lift coefficient curves, and C_{DC} is the drag coefficient of cross current

which depends on tip shape and rake ratio (e.g. Quadrate tip: $C_{DC}=0.8$. Smooth tip: $C_{DC}=0.4$). C_{d0} is the airfoil profile drag coefficient (viscous drag). For the profile section NACA0015, $C_{d0}=0.0065$. Λ is the sweptback angle at 1/4 chord of the fin. λ is the aspect ratio. α is the angle of attack (degree).

In order to get C_L and C_D , we should know the real effective angle of attack. As the fin located at some offset from the origin of the AUV coordinate system, it experiences the following effective velocities

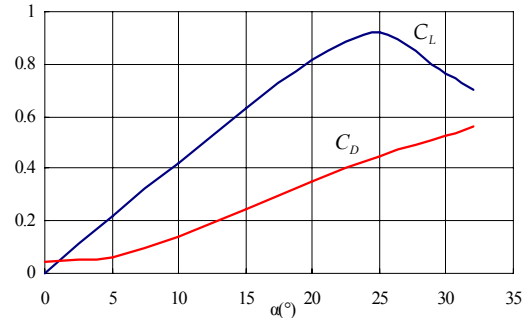


Figure 3. Lift and drag coefficient curves.

$$\begin{cases} u_{fin} = u + z_{fin}r - y_{fin}r \\ v_{fin} = v + x_{fin}r - z_{fin}p \\ w_{fin} = w + y_{fin}q - x_{fin}q \end{cases} \quad (18)$$

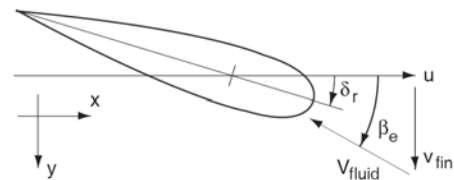
Where x_{fin} , y_{fin} and z_{fin} are the body-fixed coordinates of the fin posts.

The effective fin angles of attack δ_{se} and δ_{re} are given by

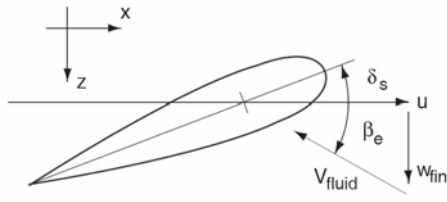
$$\begin{cases} \delta_{se} = \delta_s + \beta_{se} \\ \delta_{re} = \delta_r + \beta_{re} \end{cases} \quad (19)$$

Where δ_r and δ_s are the fin angles referenced to the vehicle hull, β_{re} and β_{se} are the effective angles of attack of the fin zero plane, as shown in Fig.4. β_{re} and β_{se} are given by

$$\begin{cases} \beta_{re} = \frac{v_{fin}}{u_{fin}} = \frac{v + x_{fin}r - z_{fin}p}{u + z_{fin}r - y_{fin}r} \\ \beta_{se} = \frac{w_{fin}}{u_{fin}} = \frac{w + y_{fin}q - x_{fin}q}{u + z_{fin}r - y_{fin}r} \end{cases} \quad (20)$$



(a) Effective rudder angle of attack



(b) Effective stern plane angle of attack
Figure 4. Effective angle of attack scheme.

Basing on the above analysis, (1) could be rewritten into more detailed form.

$$(\mathbf{M}_{RB} + \mathbf{M}_A)\dot{\mathbf{V}} = \boldsymbol{\tau}_G + \boldsymbol{\tau}_{prop} + \boldsymbol{\tau}_R + \mathbf{D}(\mathbf{V})\mathbf{V} - (\mathbf{C}_{RB}(\mathbf{V}) + \mathbf{C}_A(\mathbf{V}))\mathbf{V} \quad (21)$$

$$\mathbf{T}_1 = \begin{bmatrix} \cos \psi \cos \theta & \cos \psi \sin \theta \sin \varphi - \sin \psi \cos \varphi & \cos \psi \sin \theta \cos \varphi + \sin \psi \sin \varphi \\ \sin \psi \cos \theta & \sin \psi \sin \theta \sin \varphi + \cos \psi \cos \varphi & \sin \psi \sin \theta \cos \varphi - \cos \psi \sin \varphi \\ -\sin \theta & \cos \theta \sin \varphi & \cos \theta \cos \varphi \end{bmatrix} \quad (23)$$

$$\mathbf{T}_2 = \begin{bmatrix} 1 & \tan \theta \sin \varphi & \tan \theta \cos \varphi \\ 0 & \cos \varphi & -\sin \varphi \\ 0 & \sin \varphi \sec \theta & \cos \varphi \sec \theta \end{bmatrix} \quad (24)$$

D. Numerical Integration

Given the complex and highly nonlinear nature of (21) and (22), we will use numerical integration to solve these equations and get the vehicle speed, position, and attitude vs time.

The non-linear state equation of the AUV is given by $\dot{\mathbf{x}}_n = \mathbf{f}(\mathbf{x}_n, \mathbf{u}_n)$ (25)

Where \mathbf{x}_n is the state vector, and \mathbf{u}_n is the input vector:

$$\mathbf{x}_n = [u \ v \ w \ p \ q \ r \ \xi \ \eta \ \zeta \ \varphi \ \theta \ \psi]^T \quad (26)$$

$$\mathbf{u}_n = [\boldsymbol{\tau}_{prop} \ \boldsymbol{\tau}_R] \quad (27)$$

Here, Runge-Kutta of numerical integration is usually used to solve the equations. Firstly, we calculate the following equations

$$\begin{aligned} k_1 &= \mathbf{x}_n + \mathbf{f}(\mathbf{x}_n, \mathbf{u}_n) \\ k_2 &= \mathbf{f}(\mathbf{x} + \frac{\Delta t}{2}k_1, \mathbf{u}_{n+\frac{1}{2}}) \\ k_3 &= \mathbf{f}(\mathbf{x} + \frac{\Delta t}{2}k_2, \mathbf{u}_{n+\frac{1}{2}}) \\ k_4 &= \mathbf{f}(\mathbf{x} + \Delta tk_4, \mathbf{u}_{n+1}) \end{aligned} \quad (28)$$

Where the interpolated input vector is

$$\mathbf{u}_{n+\frac{1}{2}} = \frac{1}{2}(\mathbf{u}_n + \mathbf{u}_{n+1}) \quad (29)$$

Then, we combine the above equations

$$\mathbf{x}_{n+1} = \mathbf{x}_n + \frac{\Delta t}{6}(k_1 + 2k_2 + 2k_3 + k_4) \quad (30)$$

E. Simulation and Comparison

Basing on the above mathematic modelling and analysis, we build the simulation system of WL-II mini-

C. Kinematics Model

The coordinate transformation between body-fixed coordinate system and inertial coordinate system can be given by

$$\begin{bmatrix} \dot{\xi}_G \\ \dot{\eta}_G \\ \dot{\zeta}_G \\ \dot{\varphi} \\ \dot{\theta} \\ \dot{\psi} \end{bmatrix} = \begin{bmatrix} \mathbf{T}_1 & \mathbf{0}_{3 \times 3} \\ \mathbf{0}_{3 \times 3} & \mathbf{T}_2 \end{bmatrix} \begin{bmatrix} u \\ v \\ w \\ p \\ q \\ r \end{bmatrix} \quad (22)$$

Where ξ_G , η_G and ζ_G are the barycentre coordinates in inertial coordinate system, \mathbf{T}_1 and \mathbf{T}_2 are coordinate transform matrix given by

AUV [12]. We can obtain the present relative acceleration of the AUV in the global coordinates, and the velocity of the next moment through Runge-Kutta numerical integral, and the displacement of the next moment further. The operating flowchart is shown in figure 5. The visual simulation system is shown in figure 6.

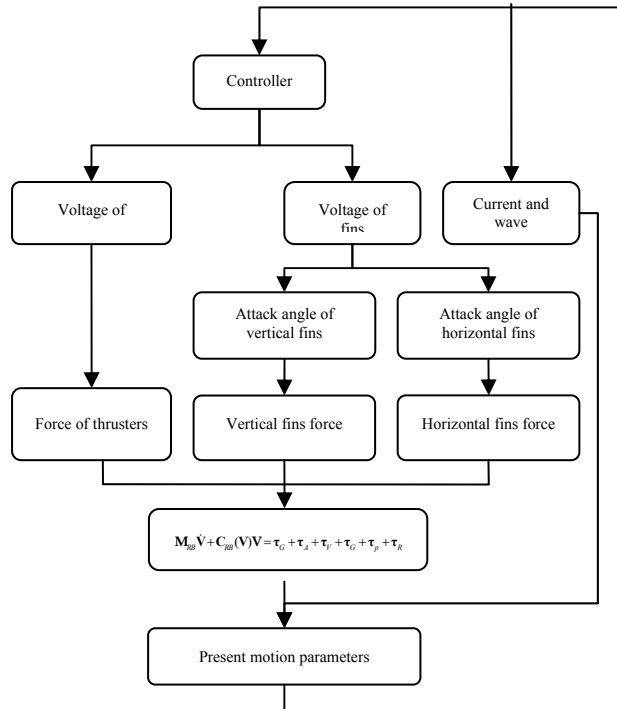


Figure 5. Operating flowchart of the simulation system.

The simulation results are compared with the results of at-sea experiments. The zigzag-like motions in horizontal plane and vertical plane are simulated and the Comparisons are shown in figure 7.

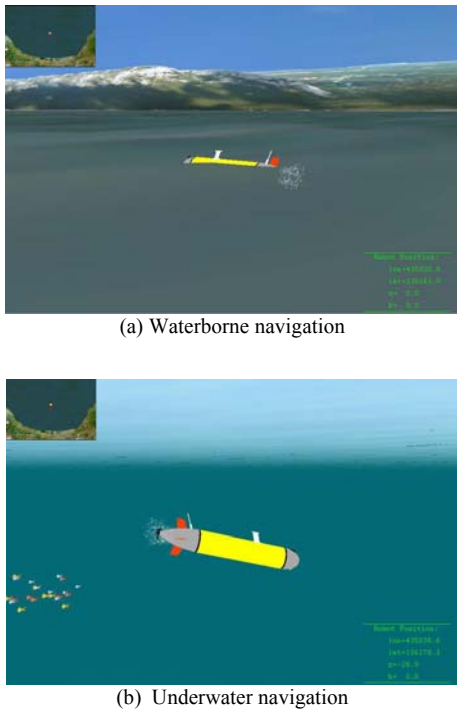


Figure 6. Visual simulation system of WL-II mini-AUV.

From the comparison between simulation results and experiment results, we can conclude that the mathematic model of the AUV motion and the numerical integration method are accurate and feasible.

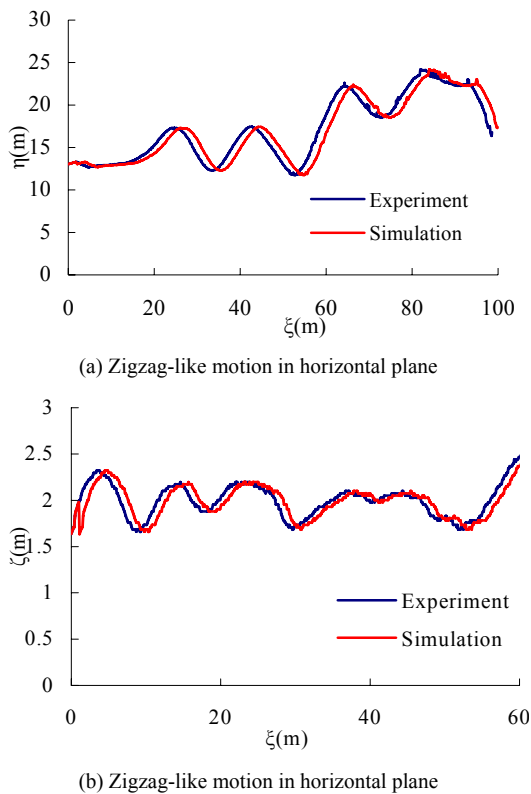


Figure 7. Comparison of simulation results.

CONCLUSION

This paper concentrates on the problem of dynamic modeling for the AUV with fins. Firstly, we build motion equation in 6-DOF and analyze the force and hydrodynamic coefficients in detail, especially the fin effect. We build the simulation system according to deduction of the proposed mathematical model. The feasibility and accuracy are verified by comparing the results between at-sea experiments and simulation for WL-II mini-AUV. The results verify the feasibility and the superiority of the mathematical modeling. Moreover, the model and simulation system can be used universally to most AUVs with fins.

ACKNOWLEDGMENT

This work is supported by the National Natural Science Foundation of China (Grant No. 51209025) and the China Postdoctoral Science Foundation (Grant No. 20110491519) and Fundamental Research Funds for the Central Universities of China (Grant No. 017284, 2011QN130) and Special Fund for Marine Scientific Research in the Public Interest (Grant No.201005010).

REFERENCES

- [1] Blidberg D.R., "Autonomous underwater vehicles: a tool for the ocean," *Unmanned Systems*, vol. 9, no. 2, pp. 10-15, 1991.
- [2] Xu YuRu, Pang Y.J., Gan Y. and Sun Y.S. , "AUV-state-of-the-art and prospect," *CAAI Transactions on Intelligent Systems*, vol.1, no.1, pp. 9-16, September 2006.
- [3] Xu YuRu and Xiao Kun, "Technology development of autonomous ocean vehicle," *Journal of Automation*, vol. 33, no. 5, pp. 518-521, 2007.
- [4] Conte G. and Serrani A., "Modeling and simulation of underwater vehicles," *Proceedings of the 1996 IEEE International Symposium on Computer-Aided Control System Design*, pp. 62-67, Dearborn, Michigan, September 1996.
- [5] Timothy P., "Development of a Six-Degree of Freedom Simulation Model for the REMUS Autonomous Underwater Vehicle: Oceans," *MTS/IEEE Conference and Exhibition*, pp. 450-455, May 2001.
- [6] Prestero T. J., "Development of a six-degree of freedom simulation model for the REMUS autonomous underwater vehicle," *Proceedings of the OCEANS 2001 MTS/IEEE Conference and Exhibition*, pp. 450-455, Honolulu, Hawaii, November 2001.
- [7] Ridley P., Fontan J. and Corke P., "Submarine dynamic modeling," *Proceedings of the Australian Conference on Robotics and Automation*, Brisbane, Australia, December 2003.
- [8] Chang Wenjun, Liu Jiancheng and Yu Huanan, "Mathematic model of the AUV motion control and simulator," *Ship Engineering*, vol.12, no.3, pp. 58-60, September 2002.
- [9] Li Ye, Liu Jiancheng and Shen Mingxue, "Dynamics model of underwater robot motion control in 6 degrees of freedom," *Journal of Harbin Institute of Technology*, vol.12, no.4, pp. 456-459, December 2005.
- [10] Nahon M., "A Simplified Dynamics Model for Autonomous Underwater Vehicles," *Journal of Ocean Technology*, vol. 1, no. 1, pp. 57-68, 2006.

- [11] Silva J., Terra B., Martins R. and Sousa J., "Modeling and Simulation of the LAUV Autonomous Underwater Vehicle," *Proceedings of the 13th IEEE IFAC International Conference on Methods and Models in Automation and Robotics*, pp. 713-718, Szczecin, Poland, August 2007.
- [12] Su Yumin, Wan Lei and Li Ye, "Development of a small autonomous underwater vehicle controlled by thrusters and fins," *Robot*, vol. 29, no. 2, pp. 151-154, 2007.
- [13] Shi Shengda, *Submarine Maneuverability*. National Defence Industry Press, Beijing, 1995.
- [14] Louis A.G., "Design, modelling and control of an autonomous underwater vehicle," *Bachelor of engineering honours thesis*, University of Western Australia, 2004.
- [15] Bing Zhu, Xu-yan Zhou, Bin Tan, "Algorithm for Detecting the Image of River Sediment Based on Hydrometric Cableway", *Journal of Software*, vol. 6, no. 8, pp. 1437-1444, 2011.
- [16] Yasser Mohamed Abd El-Lati, "A New Model for the Structure of Leaves", *Journal of Software*, vol. 6, no. 4, pp. 662-669, 2011



Xiao Liang was born in 1980. He received doctor degree in Design and Construction of Naval Architecture and Ocean Structure, Harbin Engineering University, Harbin, China, 2009. His major field of study is hydrodynamics and underwater vehicles.

He has published more than 20 papers in journals and conferences. One of his current jobs is Reliability Analysis of AUV Control System cooperating with State Key Laboratory of AUV, China. His current research interests include modeling, simulation and intelligent control of the AUV with fins.

Dr. Liang is the senior member of International Association of Computer Science and Information Technology, and the member of Royal Institute of Naval Architect.



Jundong Zhang was born in 1967. He received his doctor degree in Marine Engineering, Dalian Maritime University, Dalian, China, 1998. His major field of study is simulation and motion control of ship and marine engine.

He has been worked in Dalian Maritime University since 1982. Now, he is a professor and doctoral supervisor in Marine Engineering, and he is the principal of marine engineering discipline in Dalian Maritime University. He has published more than 50 papers in journals and conferences, and he has written 5 books. One of his current jobs is Design of Marine Engineering Simulator cooperating with some universities or companies. His current research interests include modeling and simulation of ship marine engine.

Prof. Zhang is the senior member of Chinese Society of Naval Architecture and Marine Engineering, also the senior member of Chinese Navigation Society.